

## ARTICLE



# STAT3-mediated transactivation of NOVA2 promotes lung adenocarcinoma metastasis by splicing SMAD4

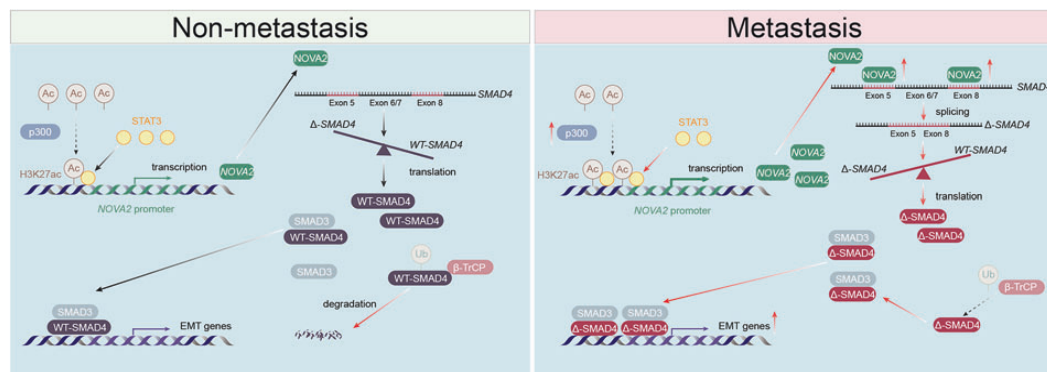
Shengjie Wang<sup>1,2,13</sup>✉, Xin Tong<sup>3,13</sup>, Runfeng Sun<sup>1,2,4,13</sup>, Xinyi Xia<sup>1,5,6,13</sup>, Donglai Chen<sup>1,7,13</sup>, Zhao Wang<sup>1,8,13</sup>, Hao Shi<sup>9,10,11</sup>, Chenzhuo Wu<sup>3</sup>, Xiaoxiao Guo<sup>1</sup>, Die Hu<sup>1</sup>, Ersuo Jin<sup>12</sup>✉ and Hong-Tao Zhang<sup>1,2,3,9,10,11</sup>✉

© The Author(s), under exclusive licence to Springer Nature Limited 2026

Metastasis remains the primary cause of mortality in lung adenocarcinoma (LUAD) patients. However, the molecular mechanisms underlying LUAD cell metastasis are only partially elucidated. Here, by performing integrated bioinformatic analysis of clinical data, RNA-binding protein (RBP) NOVA2 is identified as a pivotal LUAD metastasis-associated regulator. NOVA2 expression is elevated in metastatic LUAD tissues and correlates with poor prognosis of LUAD patients. Functionally, NOVA2 depletion suppresses epithelial-mesenchymal transition (EMT), migration, and invasion in vitro, and attenuates LUAD cell metastasis in vivo. Mechanistically, histone acetyltransferase p300 augments H3K27 acetylation level and facilitates the binding of STAT3 to the NOVA2 promoter, which in turn promotes NOVA2 transcription. Increased NOVA2 expression induces exon skipping (exons 6–7) in SMAD4 to generate a truncated splicing isoform (termed  $\Delta$ -SMAD4). The resulting  $\Delta$ -SMAD4 isoform evades E3 ubiquitin ligase  $\beta$ -TrCP-mediated ubiquitination, maintaining its ability to form complex with SMAD3 (R-SMAD) and sustain TGF- $\beta$ /SMAD signaling. Moreover, in NOVA2-overexpressing LUAD cells,  $\Delta$ -SMAD4 knockdown has stronger inhibitory effects on TGF- $\beta$ -induced EMT and invasion than does SMAD4 knockdown. In summary, our findings identify a novel mechanism by which STAT3-mediated transcriptional upregulation of NOVA2 promotes SMAD4 splicing in metastatic LUAD, and suggest that the STAT3-NOVA2- $\Delta$ -SMAD4 axis drives EMT and LUAD metastasis, which may be a promising therapeutic target for treating LUAD.

Oncogene; <https://doi.org/10.1038/s41388-026-03752-6>

## Graphical Abstract



## INTRODUCTION

Metastasis is the leading cause of cancer-related mortality, responsible for 90% of all cancer-related deaths [1]. Non-small cell lung cancer (NSCLC) carries a dire prognosis, with most cases diagnosed at advanced stages. Additionally, 50% of patients who undergo surgery for early-stage NSCLC experience recurrence or

metastasis, while fewer than 10% of patients with distant disease can survive for 5 years [2–4]. Lung adenocarcinoma (LUAD), the most prevalent histologic subtype of NSCLC, continues to have a poor prognosis due to the presence of metastatic tumors in over half of patients at the time of diagnosis [5]. Consequently, understanding the mechanisms driving LUAD metastasis is

<sup>1</sup>Department of Basic Medicine, Kangda College of Nanjing Medical University; Lianyungang Medical-Education Innovation and Research Center, Nanjing Medical University, Lianyungang, Jiangsu Province, China. <sup>2</sup>Collaborative Innovation Center of Molecular Medicine between Soochow University and Donghai County People's Hospital, Suzhou Medical College of Soochow University, Suzhou, Jiangsu Province, China. <sup>3</sup>Department of Thoracic Surgery, The First Affiliated Hospital of Soochow University, Suzhou Medical College of Soochow University, Suzhou, Jiangsu Province, China. <sup>4</sup>Donghai County People's Hospital, Lianyungang, Jiangsu Province, China. <sup>5</sup>Institute of Laboratory Medicine, Nanjing Jinling Hospital, The Affiliated Hospital of Medical School, Nanjing University, Nanjing, Jiangsu Province, China. <sup>6</sup>State Key Laboratory of Analytical Chemistry for Life Science, Nanjing University, Nanjing, Jiangsu Province, China. <sup>7</sup>Department of Thoracic Surgery, Zhongshan Hospital, Fudan University, Shanghai, China. <sup>8</sup>Department of Oncology, The First Affiliated Hospital of Soochow University, Suzhou Medical College of Soochow University, Suzhou, Jiangsu Province, China. <sup>9</sup>Department of Medical Genetics, School of Basic Medical Sciences, Suzhou Medical College of Soochow University, Suzhou, Jiangsu Province, China. <sup>10</sup>Soochow University Laboratory of Cancer Molecular Genetics, Suzhou Medical College of Soochow University, Suzhou, Jiangsu Province, China. <sup>11</sup>Suzhou Key Laboratory for Molecular Cancer Genetics, Suzhou, Jiangsu Province, China. <sup>12</sup>Department of Cell Biology, College of Medicine, Jiaxing University, Jiaxing, Zhejiang Province, China. <sup>13</sup>These authors contributed equally: Shengjie Wang, Xin Tong, Runfeng Sun, Xinyi Xia, Donglai Chen, Zhao Wang. ✉email: [wsj1088@njmu.edu.cn](mailto:wsj1088@njmu.edu.cn); [ersuojin@zjxu.edu.cn](mailto:ersuojin@zjxu.edu.cn); [htzhang@suda.edu.cn](mailto:htzhang@suda.edu.cn)

Received: 17 September 2025 Revised: 27 February 2026 Accepted: 13 March 2026

Published online: 01 April 2026

essential for the identification of predictive biomarkers and the development of novel therapeutic targets to improve patient outcomes.

LUAD is characterized by remarkable molecular diversity and the presence of diverse oncogenic driver mutations [6]. Notably, tumor suppressor genes and proto-oncogenes are particularly susceptible to splicing defects, and aberrantly expressed splicing factors can exhibit oncogenic properties [7]. Alternative splicing (AS) increases the proteomic and transcriptomic diversity derived from a limited number of genomic loci [8], and its dysregulation contributes to a range of diseases, from developmental disorders to cancer [9]. In cancer, aberrant splicing fuels therapy resistance, tumor progression, and metastasis through the generation of oncogenic isoforms [10–12]. RNA-binding proteins (RBPs) are central regulators of RNA splicing, binding to pre-mRNA to control the differential inclusion or exclusion of exons and introns during mRNA maturation. RBP-mediated AS plays a critical role in mRNA stability and protein diversity [13]. The dysregulation or malfunction of RBPs results in unbalanced expression of key oncogenes and tumor-suppressor genes, thereby influencing cancer phenotypes, particularly metastasis [14]. Given that splicing dysregulation is a hallmark of cancer [15], RBP-mediated splicing alterations can provide a selective advantage to tumor cells and present potential therapeutic targets.

The NOVA family, comprising neuron-specific KH-type RBPs such as NOVA1 and NOVA2, is well-known for its role in regulating AS and polyadenylation by binding to YCAY motifs [16]. NOVA2 is crucial in RNA splicing, binding to YCAY clusters of pre-mRNAs and assembling spliceosomes to modulate the inclusion or exclusion of exons and introns, thereby influencing mRNA development [17]. NOVA2 is implicated in various diseases, with NOVA splicing factors playing significant roles not only in the physiology of neurons and certain non-neuronal cells but also in related diseases, including neurological disorders and a broad range of cancers [17, 18]. Specifically, NOVA2-mediated AS programs contribute to cancer progression by regulating angiogenesis in colon cancer and ovarian cancer [19, 20]. However, the mechanisms driving aberrant NOVA2 expression and its role in tumor metastatic progression are poorly understood.

The TGF- $\beta$  signaling pathway exhibits dual-context dependence in cancer, inhibiting proliferation in premalignant lesions while promoting metastasis in advanced tumors by regulating angiogenesis, immune evasion, and extracellular matrix remodeling [21–23]. In the canonical pathway, TGF- $\beta$  binds to its dual-specificity kinase receptor complex, composed of type II and type I receptors, which subsequently cause phosphorylation of SMAD2/SMAD3 (R-SMADs). Phosphorylated SMAD2 and/or SMAD3 then form an oligomeric complex with SMAD4, which is translocated to the nucleus, where it binds to the promoters of target genes to regulate their expression [24]. SMAD4, an essential mediator of TGF- $\beta$ /SMAD signaling pathway, undergoes dynamic post-translational modifications that fine-tune the amplitude and duration of signaling, which includes SUMOylation and ubiquitin-dependent degradation [25]. However, the mechanistic underpinnings of SMAD4 regulation in metastatic LUAD remain unclear, particularly its interaction with RBP networks that facilitate TGF- $\beta$ -induced pro-metastatic activities.

In this study, we integrate clinical data, functional genomics, and molecular profiling to unravel a NOVA2-driven axis in LUAD metastasis. We find that histone acetylation by p300 potentiates STAT3-mediated transactivation of NOVA2, which in turn increases NOVA2 protein expression and induces exons 6–7 skipping in SMAD4 mRNA. The resulting  $\Delta$ -SMAD4 isoform evades  $\beta$ -TrCP-mediated ubiquitination, leading to sustained TGF- $\beta$ /SMAD signaling activation and eventually promoting LUAD metastasis.

## MATERIALS AND METHODS

All detailed protocols were described in the Supplementary Experimental Procedures.

## RESULTS

### NOVA2 is aberrantly upregulated in metastatic LUAD and predicts an unfavorable prognosis for patients with LUAD

To investigate RBPs involved in LUAD metastasis, bioinformatics analysis was conducted by intersecting five candidate lists: (1) two established RBP databases (EuRBPDB [26] and ATtRACT [27]) for comprehensive RBP annotation; (2) LUAD-specific metastasis-associated gene repertoires from CancerSEA datasets [28]; (3) two prognostic gene signatures derived from clinical cohorts [29]. This approach identified a subset of RBPs that are both functionally relevant to metastatic processes and possess significant prognostic value (Fig. 1A). In addition to validating five transcript (CEBP4, IGF2BP1, IGF2BP3, NOVA2, and RBMS3) changes via quantitative real-time PCR experiments in LUAD cases (Fig. 1B), prognosis analysis of candidate RBPs was performed (Fig. S1A–S1E), with a specific focus on metastasis-related prognosis (Fig. S1F–S1J). Notably, only NOVA2 expression was significantly elevated in metastatic LUAD tissues compared to that in non-metastatic counterparts (Fig. 1B and Table S1) and were also associated with poor prognosis in patients with N1 stage LUAD (Fig. S1I). Consequently, NOVA2 was selected as a potential metastasis-related RBP in LUAD. Consistent with clinical observations, NOVA2 was upregulated in LUAD cell lines (A549, H1299, H1650, and H1975) relative to human bronchial epithelial cells (BEAS-2B) (Fig. S1K and S1L). Interestingly, the highly metastatic A549-M cell line showed elevated NOVA2 levels compared to the weakly metastatic A549 cell line (Fig. 1C and S1M). To assess the clinical significance of NOVA2 in patients with LUAD, NOVA2 protein expression was evaluated via immunohistochemistry (IHC) on LUAD tissue microarrays (Fig. 1D–F). IHC analysis revealed upregulation of NOVA2 in both advanced T stages and metastatic LUAD tissues (Fig. 1G, H). Moreover, high NOVA2 expression strongly correlated with poor prognosis (Fig. 1I). Collectively, these results suggest that NOVA2 may play a pivotal role in LUAD metastasis.

### NOVA2 facilitates LUAD cell EMT and metastasis

Given NOVA2's role as an RBP involved in metastatic processes and its strong association with metastases, its mechanistic role in regulating the invasive and metastatic potential of LUAD cells was explored. Stable cell lines were established *via* lentiviral infection of highly metastatic A549-M cells. Given the critical involvement of epithelial-mesenchymal transition (EMT) in tumor progression and metastasis, key EMT markers were examined following NOVA2 knockdown. Notably, significant downregulation of key EMT regulators, including Snail, MMP2, and Vimentin, was observed in NOVA2-silenced cells (Fig. 2A). In line with the suppression of EMT, silencing of NOVA2 markedly impaired migratory and invasive capacities in transwell assays (Fig. 2B, C). These findings were further validated by wound healing experiments, which revealed significantly reduced cell motility upon NOVA2 depletion (Fig. 2D, E). Furthermore, overexpression of NOVA2 promoted EMT, as indicated by downregulation of E-cadherin and upregulation of N-cadherin in A549 and H1975 cells (Fig. S2A) and NOVA2 overexpression enhanced the migratory and invasive abilities (Fig. S2B and S2C). Together, these results position NOVA2 as a pivotal regulator of EMT-driven metastatic behavior *in vitro*.

To assess the impact of NOVA2 on cell metastasis *in vivo*, A549-M cells stably expressing sh-NOVA2 or sh-NC (control), along with parental A549 cells, were injected into the lateral tail veins of BALB/c nude mice. After 6 weeks, mice were euthanized, and lungs were excised for analysis. Notably, a significant reduction in metastatic lung nodules was observed in the sh-NOVA2 group compared to controls (Fig. 2F, G). Histological analysis of lung tissues confirmed a significant decrease in micrometastatic foci injected with sh-NOVA2 (Fig. 2H–J). To validate this, we performed the tail vein injection of NOVA2-overexpressing H1975 cells in BALB/c nude mice. As a result, NOVA2 overexpression increased

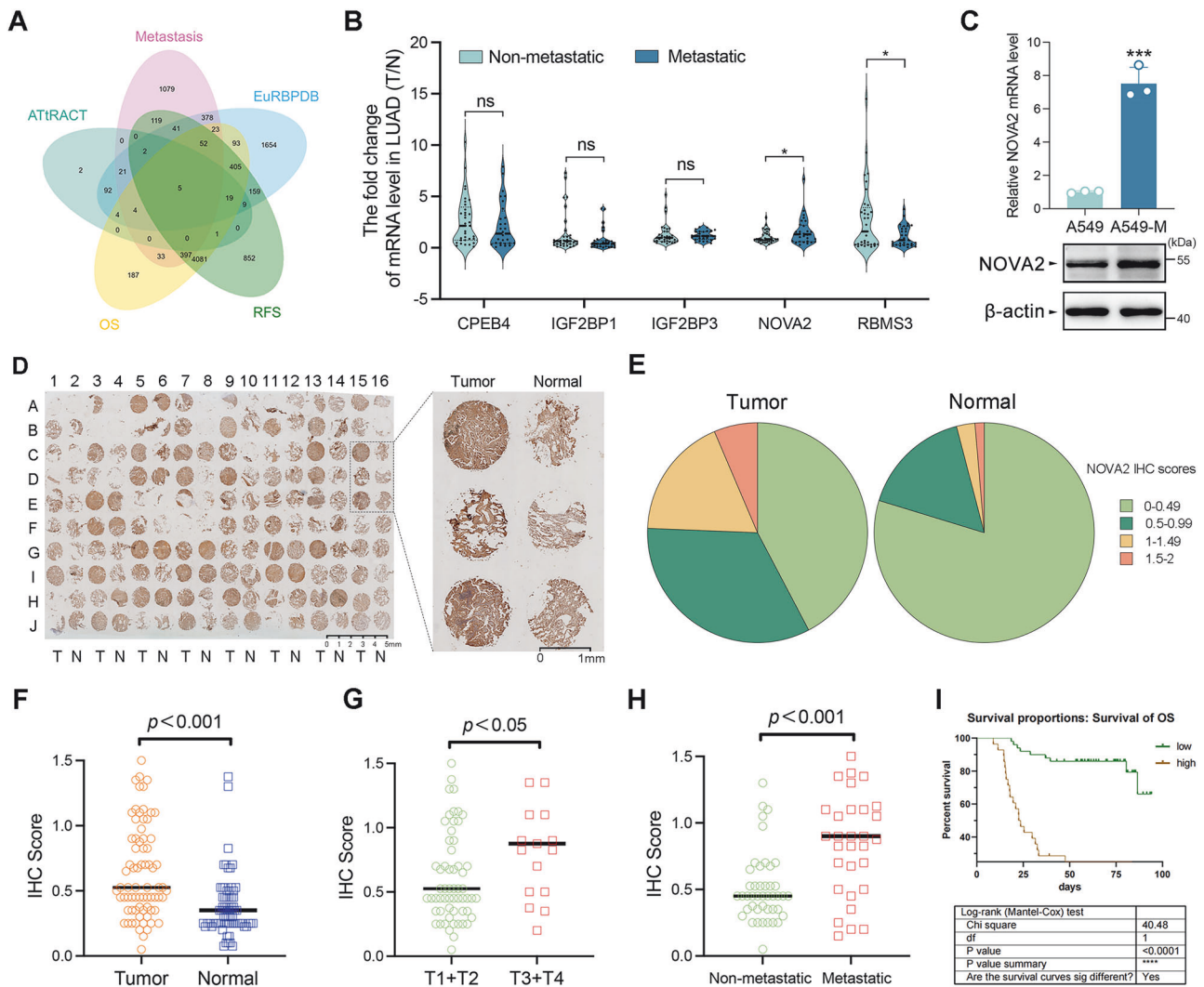


**Fig. 1 Identification of metastatic LUAD-associated NOVA2.** **A** Two LUAD overall survival (OS) and recurrence-free survival (RFS) cohort datasets were integrated with human RBP databases (ATTRACT/EuRBPDB) and LUAD metastasis gene signatures (CSEA) to identify metastasis-associated RBPs. Venn analysis identified consensus candidates across all five datasets. **B** Relative mRNA expression (T/N) of five RBPs in metastatic ( $n = 28$ ) and non-metastatic ( $n = 33$ ) LUAD tissues. LUAD tissues were categorized into metastatic and non-metastatic groups as described in “Materials and Methods”; T, LUAD tissues; N, paracarcinoma tissues. The Y-axis represents the fold change in mRNA expression (T/N) for each of the five RBPs as indicated. Data are shown as the mean  $\pm$  SD of  $n = 3$  biological replicates. ns, not significant; \* $P < 0.05$  by unpaired Student's *t* test. **C** Expression of NOVA2 mRNA in highly metastatic A549-M cells and low-metastatic A549 cells. Data are shown as the mean  $\pm$  SD of  $n = 3$  biological replicates. \*\*\* $P < 0.001$  by unpaired Student's *t* test. **D** NOVA2 protein expression was analyzed by immunohistochemistry on LUAD tissue microarrays. Scale bar, 1 mm. **E** Pie charts illustrating the distribution of NOVA2 IHC scores in LUAD and paracarcinoma normal tissues. **F** IHC scores of NOVA2 in LUAD tissue microarrays and matched paracarcinoma tissues. Tumor, LUAD tissues; Normal, paracarcinoma tissues. **G, H.** High NOVA2 expression was significantly associated with advanced T stage and metastasis (lymph node and/or distal metastasis). **I** Kaplan–Meier analysis of OS for patients with LUAD (low vs. high NOVA2 expression). Data are shown as the mean  $\pm$  SD. \*\*\*\* $P < 0.0001$  by unpaired Student's *t* test.

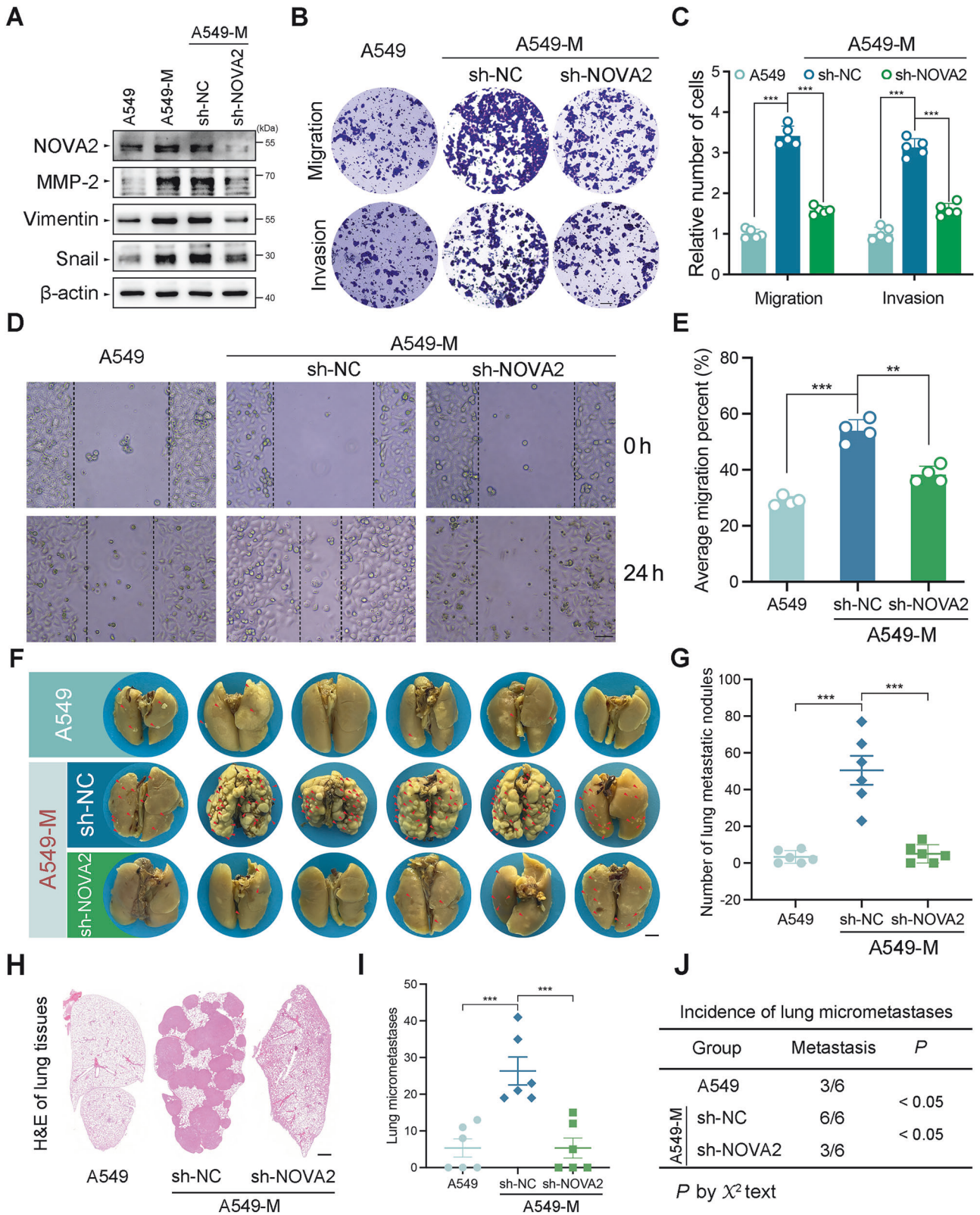
pulmonary metastatic capacity (Fig. S2D and S2E). These results collectively demonstrate that NOVA2 plays a metastasis-driving role in LUAD cells.

#### STAT3 promotes NOVA2 transcriptional activity in LUAD cells

Gene expression is intricately regulated epigenetically by DNA modification and histone modification [30], transcriptionally by transcription factors (TFs) [31], and post-transcriptionally by RNA sequence/structure, miRNAs, and external factors (e.g., pH; oxidative stress) [32–34]. To identify potential TFs driving aberrant NOVA2 expression, we performed an integrative analysis of four TF prediction databases (hTFtarget, FIMO\_JASPAR, ChIP-Atlas, and KnockTF). Intersection of these datasets revealed two candidate regulators: signal transducer and activator of transcription 3

(STAT3) and transcription factor AP-2 gamma (TFAP2C) (Fig. 3A). Functional validation through RNA interference demonstrated that STAT3 knockdown significantly reduced NOVA2 mRNA levels in both A549 parental cells and A549-M subline (Fig. 3B and S3A), while TFAP2C silencing had no measurable effect (Fig. 3C and S3B). Notably, STAT3 knockdown also led to a reduction in NOVA2 protein expression in two cell models (Fig. 3D). Clinically, patients with LUAD high STAT3 expression experienced significantly shorter overall survival compared to those with low STAT3 expression, whereas TFAP2C expression showed no significant association with patient survival (Fig. S3C and S3D). Moreover, only STAT3 exhibited a significant positive correlation with NOVA2 expression in LUAD samples (Fig. S3E and S3F). To determine whether STAT3 directly regulates NOVA2 expression,





its promoter region was analyzed by cloning a 2,229 bp genomic fragment (-2,228 to 0 bp relative to the transcription start site) into the pGL3-basic luciferase reporter vector. STAT3 knockdown specifically reduced reporter activity (Fig. 3E), prompting further analysis of the *NOVA2* promoter for potential STAT3 binding sites.

Bioinformatic prediction of STAT3 binding motifs (JASPAR ID: MA0144.3) (Fig. 3F) led to the design of five progressive 5'-deletion constructs spanning the -2228 bp of *NOVA2* promoter region. Luciferase reporters containing promoter fragments lacking -412~0 bp region did not respond to STAT3, suggesting



**Fig. 2 NOVA2 promotes LUAD cell EMT and metastasis.** **A** Immunoblotting analysis of MMP2, Vimentin, and Snail protein expression in A549 and NOVA2-silenced A549-M cells.  $\beta$ -actin served as the loading control. **B, C** Transwell migration and invasion assays performed in stable NOVA2-silenced A549-M cells. Migrated and invasive cells were stained, photographed, and counted in at least four random fields under a light microscope. Representative images (B) and the relative number of migrated and invasive cells (C) are presented. Scale bar, 100  $\mu$ m. Data are presented as the mean  $\pm$  SD of  $n = 5$  biological replicates.  $***P < 0.001$  by unpaired Student's  $t$  test. **D, E** Wound-healing migration assays performed in NOVA2-silenced A549-M cells and control cells. Scale bar, 100  $\mu$ m. Data are presented as the mean  $\pm$  SD of  $n = 4$  biological replicates.  $**P < 0.01$ ,  $***P < 0.001$  by unpaired Student's  $t$  test. **F** Representative images of lung metastatic nodules observed in nude mice 6 weeks after injection of NOVA2-silenced A549-M or control A549 cells. Lungs were surgically resected and stained as described in "Materials and Methods". Red arrowheads indicate metastatic nodules in the lungs. Scale bar, 5 mm. **G** Comparison of the number of lung metastatic nodules between the A549 group and the A549-M group (sh-NC, sh-NOVA2). Data are presented as the mean  $\pm$  SD of  $n = 6$  biological replicates.  $***P < 0.001$  by unpaired Student's  $t$  test. **H** H&E staining was used to evaluate lung micrometastases. Representative images showing micrometastases in lung tissues from a pair of mice as referenced in (G). Scale bar, 3 mm. **I** Quantification of micrometastases counts in lung tissues from a pair of mice referenced in (G). Data are presented as the mean  $\pm$  SD of  $n = 6$  biological replicates.  $***P < 0.001$  by unpaired Student's  $t$  test. **J** Statistical analysis of lung metastasis in the A549-M group (sh-NC, sh-NOVA2) and A549 groups.

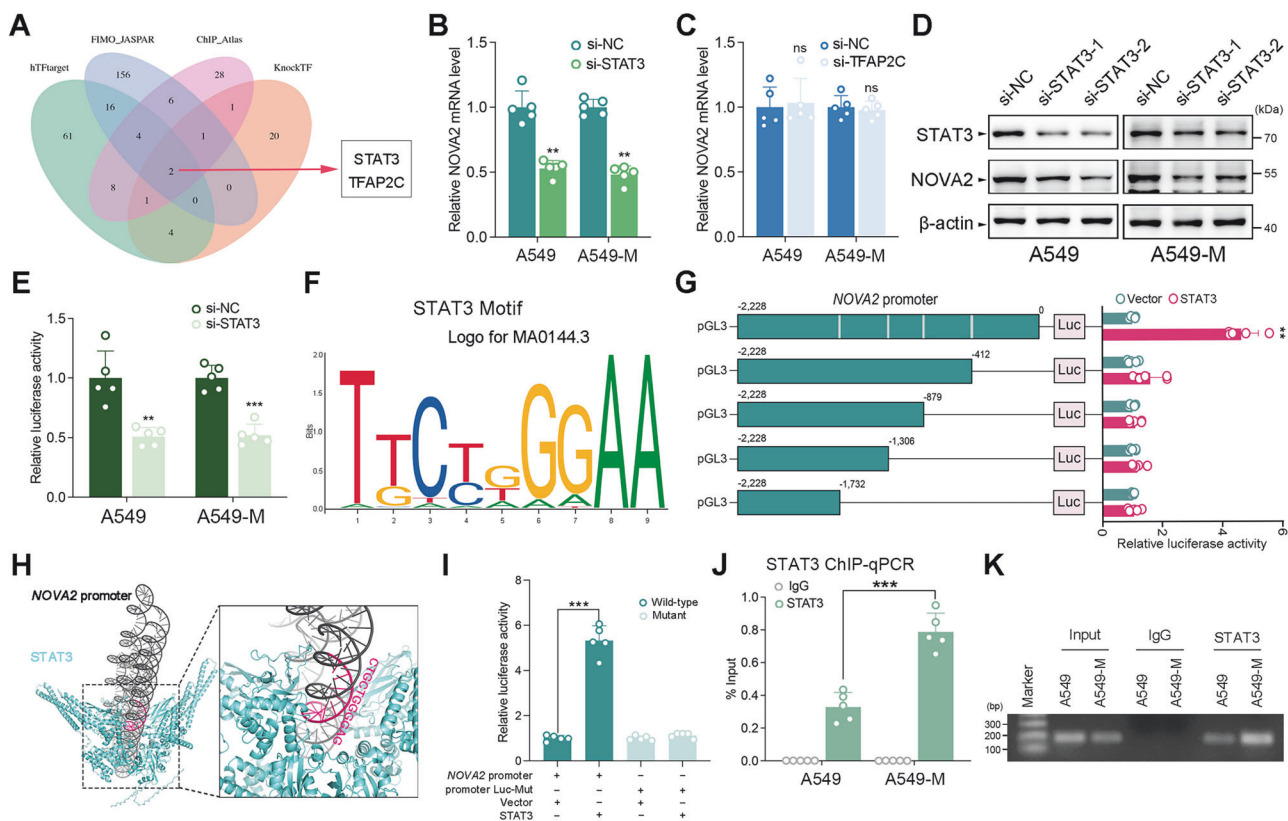


**Fig. 3 STAT3 promotes NOVA2 transcriptional activity in LUAD cells.** **A** Four TF databases (hTFtarget, FIMO\_JASPAR, ChIP-Atlas, and KnockTF) were intersected to identify potential transcription factors (TFs). The Venn diagram shows the overlap across these four datasets. **B, C** qRT-PCR analysis of NOVA2 mRNA expression in A549 and A549-M cells transfected with STAT3 siRNAs (B) or TFAP2C siRNAs (C). Data are presented as the mean  $\pm$  SD of  $n = 5$  biological replicates. ns, not significant;  $**P < 0.01$  by unpaired Student's  $t$  test. **D** Immunoblotting analysis of NOVA2 protein levels in STAT3-silenced A549 and A549-M cells. **E** Luciferase activity of the 2.2-kb NOVA2 promoter in A549 and A549-M cells transfected with STAT3 siRNAs. Data are presented as the mean  $\pm$  SD of  $n = 5$  biological replicates.  $**P < 0.01$ ,  $***P < 0.001$  by unpaired Student's  $t$  test. **F** Consensus STAT3-binding sequence used for prediction (source: <http://jaspar.genereg.net/>). **G** Identification of crucial STAT3-binding sites in the NOVA2 promoter. Diagrams of the full-length 2.2-kb NOVA2 promoter and its deletion fragments according to the STAT3 motif (left part); Luciferase activity of the full-length or four different truncated promoters in A549 cells overexpressing STAT3 (right part). Data are presented as the mean  $\pm$  SD of  $n = 5$  biological replicates.  $**P < 0.01$  by unpaired Student's  $t$  test. **H** In silico promoter analysis (AlphaFold3) identified potential STAT3-binding sites (gray-shaded region) in the NOVA2 promoter region (-412 ~ 0 bp). Structure visualization was carried out using PyMol software (source: <https://pymol.org/>). **I** Luciferase activity of the 2.2-kb NOVA2 promoter, with or without a mutation in the critical STAT3-binding site, in STAT3-overexpressing A549 cells. Data are presented as the mean  $\pm$  SD of  $n = 5$  biological replicates.  $***P < 0.001$  by unpaired Student's  $t$  test. **J, K** Anti-STAT3 ChIP assays were conducted to determine the binding of STAT3 to the NOVA2 promoter. ChIP products were amplified by qPCR (J) and RT-PCR (K) in A549 and A549-M cells. Data are presented as the mean  $\pm$  SD of  $n = 5$  biological replicates.  $***P < 0.001$  by unpaired Student's  $t$  test.

the presence of a critical STAT3-binding site within this region (Fig. 3G). Building on the observation that STAT3 impaired NOVA2 promoter activity of -2,228 ~ -412 bp region, AlphaFold3 was employed to predict potential STAT3 binding sites (Fig. 3H). Mutating this element blocked STAT3's ability to enhance

luciferase activity (Fig. 3I and S3G). To elucidate the mechanism underlying NOVA2 upregulation in metastatic LUAD, STAT3 expression was assessed in both clinical and cellular models. Surprisingly, significant differences in STAT3 levels were neither observed between metastatic and non-metastatic LUAD tissues

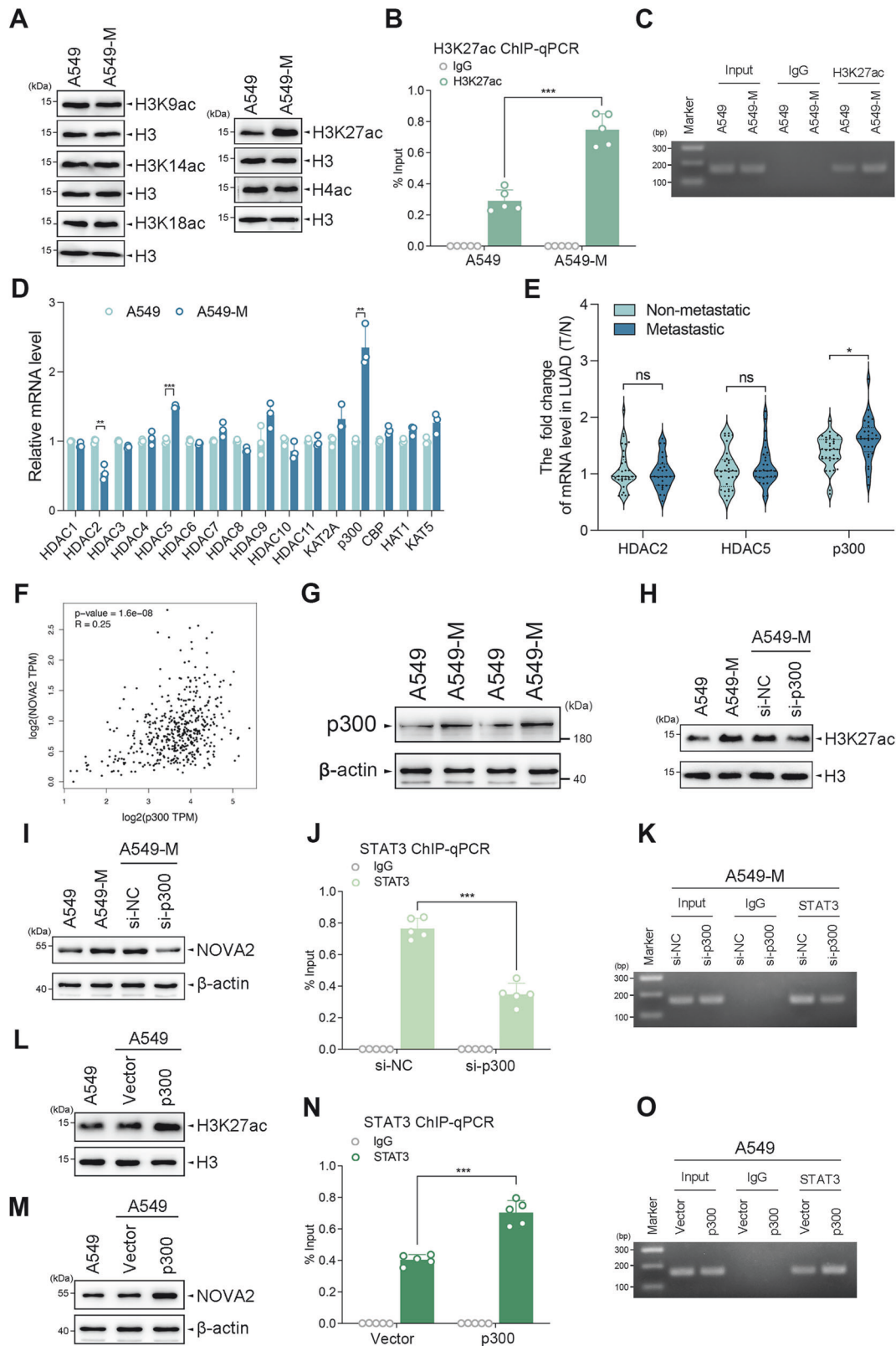


(Fig. S3H and Table S1), nor between highly metastatic and parental cell lines (Fig. S3I), being consistent with our previous research [35]. These data suggest that STAT3's role in NOVA2 activation is independent of its expression levels. Instead,

chromatin immunoprecipitation (ChIP) assays revealed enhanced binding of STAT3 to the NOVA2 promoter in metastatic LUAD, indicating that altered transcriptional regulation, rather than protein abundance, drives NOVA2 dysregulation (Fig. 3J and 3K).

**Fig. 4 p300 upregulation enhances the binding of STAT3 to NOVA2 promoter.** **A** Immunoblotting analysis of H3K9ac, H3K14ac, H3K18ac, H3K27ac, and H4ac protein expression in A549 and A549-M cells. Representative blots from three independent experiments are presented. **B, C** ChIP assays for the binding of H3K27ac to the STAT3-binding site in the NOVA2 promoter. ChIP products were amplified by qPCR (B) and RT-PCR (C) in A549 and A549-M cells. Data are presented as the mean  $\pm$  SD of  $n = 5$  biological replicates. \*\*\* $P < 0.001$  by unpaired Student's  $t$  test. **D** qPCR analysis of HDAC1-11, KAT2A, p300, CBP, HAT1, and KAT5 expression in A549 and A549-M cells. Data are presented as the mean  $\pm$  SD of  $n = 3$  biological replicates. \*\* $P < 0.01$ , and \*\*\* $P < 0.001$  by unpaired Student's  $t$  test. **E** Relative mRNA expression (T/N) of HDAC2, HDAC5, and p300 in metastatic ( $n = 28$ ) and non-metastatic ( $n = 33$ ) LUAD tissues. LUAD tissues were classified into metastatic and non-metastatic groups as described in "Materials and Methods": T, LUAD tissues; N, paracarcinoma tissues. The Y-axis represents the fold change in mRNA expression (T/N) of HDAC2, HDAC5, and p300. Data are presented as the mean  $\pm$  SD of  $n = 3$  biological replicates. ns, not significant; \* $P < 0.05$  by unpaired Student's  $t$  test. **F** Correlation analysis between p300 and NOVA2 expression in LUAD using GEPIA. **G** Immunoblotting analyses of p300 expression in A549 and A549-M cells.  $\beta$ -actin was used as loading control. **H, I** A549-M cells were transfected with control siRNA or p300 siRNA, followed by immunoblotting assays to detect H3K27ac (H) and NOVA2 (I) expression. **J, K** Anti-STAT3 ChIP assays were performed to determine the binding of STAT3 to the NOVA2 promoter. ChIP products were amplified by qPCR (J) and RT-PCR (K) in p300-silenced A549-M cells. Data are presented as the mean  $\pm$  SD of  $n = 5$  biological replicates. \*\*\* $P < 0.001$  by unpaired Student's  $t$  test. **L, M** A549 cells were transfected with p300-expressing plasmids or an empty vector. Immunoblotting assays were conducted to detect H3K27ac (L) and NOVA2 (M) expression. **N, O** Anti-STAT3 ChIP assays for the binding of STAT3 to the NOVA2 promoter. ChIP products were amplified by qPCR (N) and RT-PCR (O) in p300-overexpressing A549 cells. Data are presented as the mean  $\pm$  SD of  $n = 5$  biological replicates. \*\*\* $P < 0.001$  by unpaired Student's  $t$  test.

### p300 upregulation enhances the binding of STAT3 to NOVA2 promoter

Chromatin modifications play a pivotal role in regulating gene expression, particularly histone acetylation, which is preferentially associated with open chromatin configurations and transcriptionally active genomic regions [36]. Therefore, the protein levels of acetylated histone isoforms in A549 and A549-M cells were measured. Compared to the A549 parental cells, only H3K27ac protein levels were significantly upregulated in A549-M cells, while other acetylated histones H3K9ac, H3K14ac, H3K18ac and H4ac showed no significant changes (Fig. 4A). ChIP assays confirmed the hyperacetylation of H3K27 in the NOVA2 promoter region (Figs. 4B and C). It was understood that histone acetylation and deacetylation are regulated by histone acetyltransferases (HATs) and histone deacetylases (HDACs), respectively, where HATs acetylate histones and HDACs remove acetyl groups. Thus, we examined the expression levels of 16 specific histone acetylases in A549 and A549-M cells. qPCR analysis revealed a significant decrease in HDAC2 mRNA expression and increase in HDAC5 and p300 mRNA expression in A549-M cells (Fig. 4D). However, only p300 expression was significantly increased in metastatic LUAD tissues (Fig. 4E and Table S1). Then, TCGA data were analyzed using GEPIA, revealing a robust co-expression pattern between p300 and NOVA2 (Fig. 4F). Aberrantly increased p300 expression was observed in A549-M cells (Fig. 4G), supporting the hypothesis that p300-driven H3K27 acetylation regulates NOVA2 transcription. Genetic perturbation experiments showed that p300 knockdown decreased the expression of H3K27ac and NOVA2 (Fig. 4H, I). ChIP-qPCR assays confirmed that p300 knockdown markedly diminished the binding of STAT3 to the NOVA2 promoter (Fig. 4J, K). p300-overexpressing A549 cells exhibited substantial increased levels of H3K27ac and NOVA2 protein (Fig. 4L, M), as well as enhanced STAT3 binding to the NOVA2 promoter (Fig. 4N, O). Collectively, these results establish p300 as a pivotal epigenetic regulator of LUAD metastasis, orchestrating NOVA2 transcription through H3K27ac-dependent chromatin remodeling and facilitating STAT3-mediated transcriptional activation of NOVA2.

### NOVA2 is involved in TGF- $\beta$ signaling pathway

To elucidate the molecular mechanisms underlying NOVA2-driven metastasis in LUAD cells, RNA sequencing (RNA-seq) was performed to analyze transcriptional changes in NOVA2-overexpressing A549 cells. The RNA-seq revealed significant transcriptomic alterations, identifying 686 downregulated and 461 upregulated genes (Fig. 5A and Table S2). Gene set enrichment analysis (GSEA) of these differentially expressed genes (DEGs) highlighted TGF- $\beta$ , PI3K-AKT and Notch signaling pathway as the top-ranked pathway associated with NOVA2 overexpression (Fig. 5B, C). However, NOVA2-overexpressing A549 and H1975 cells

showed no significant differences in the overall activity of these pathways compared with control cells (Fig. S4). Considering the possibility that the crosstalk between these signaling pathways in NOVA2 overexpression, TGF- $\beta$  signaling was selected for validation. qPCR analysis validated the consistent expression changes in the top-ranked genes following NOVA2 overexpression (Fig. 5D, E). To delineate NOVA2's functional role in TGF- $\beta$  signaling, immunoblotting analyses were performed in A549 and H1975 cells with TGF- $\beta$ 1 stimulation. Interestingly, NOVA2 overexpression or silencing did not affect SMAD3 phosphorylation (p-SMAD3) and total SMAD3 protein levels (Fig. 5F–I). However, significant dysregulation of key TGF- $\beta$ /SMAD signaling targets, including *PAI-1*, *Slug*, *CDH1*, and *CDH2*, was observed in NOVA2-overexpressing cells (Fig. 5J). Taken together, these results suggest that NOVA2 modulates TGF- $\beta$  signaling through an SMAD3 phosphorylation-independent mechanism, likely by regulating the expression of downstream effectors and influencing other key regulators of TGF- $\beta$  signaling pathway.

### NOVA2 regulates SMAD4 mRNA splicing to facilitate TGF- $\beta$ -induced EMT and invasion in LUAD

Given that human NOVA2 is an RNA-binding splicing regulator, it was hypothesized that NOVA2 may regulate RNA splicing, particularly of key TGF- $\beta$  signaling regulators [37]. Genome-wide splicing analysis of NOVA2-overexpressing A549 cells identified more than one thousand differentially spliced events (Fig. 6A). Based on the aforementioned findings, attention was directed toward TGF- $\beta$ , PI3K-AKT, and Notch signaling-associated molecules. In fact, splicing analysis indicated no core genes in Notch, or PI3K-AKT pathways showing comparable splicing changes (Table S3). However, NOVA2 overexpression induced significant alterations in the splicing patterns of SMAD4 transcript, indicated by a pronounced decrease in exon 6–7 inclusion and enhanced utilization of the exon 5–8 junction (Fig. 6B). Thus, the isoform-specific PCR primers were designed, revealing two distinct bands through agarose gel electrophoresis (Fig. 6C, left panel). Sanger sequencing confirmed that the larger PCR product corresponded to SMAD4 with exon 6–7 inclusion, while the smaller PCR product, which had skipped 237 nucleotides, represented the exon 5–8 junction (Fig. 6C, right panel). Skipping of exons 6 and 7 led to an in-frame deletion of amino acids 223–302 in the linker region, generating a frameshift mutation (W302R). We conducted immunoblotting analysis using anti-SMAD4 antibodies, mapped to residues surrounding wild-type SMAD4 S315, identified a 55 kDa protein in NOVA2-overexpressing and A549-M cells, which was termed as  $\Delta$ -SMAD4 isoform lacking exon 6–7 (Fig. 6D), and the full-length SMAD4 (WT-SMAD4) with a molecular weight of  $\sim$ 61 kDa. Anti-NOVA2 RIP analysis revealed that NOVA2 predominantly binds to mRNAs of SMAD4, particularly to exons and



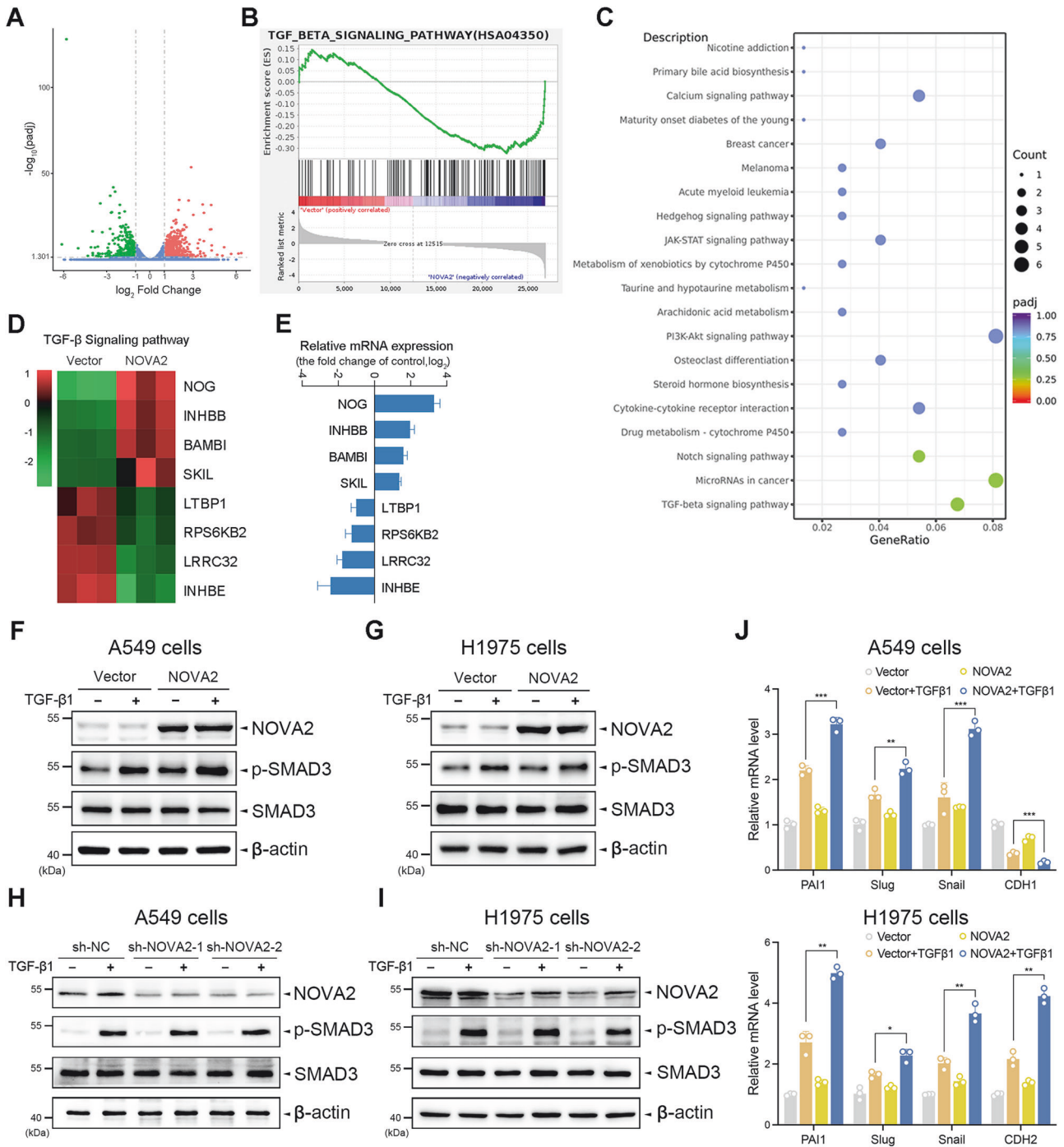


**Fig. 5 NOVA2 is involved in TGF- $\beta$  signaling pathway.** **A** Volcano plots showing the number of DEGs in A549 cells overexpressing NOVA2. **B** Gene set enrichment analysis (GSEA) of gene signatures in the control group versus NOVA2-overexpressing A549 group. Higher scores indicate a greater likelihood that the treatment positively affects the associated gene category. **C** Functional annotation clustering of genes regulated by NOVA2 overexpression in A549 cells. This enrichment was derived from a GSEA, where genes were ranked based on the  $P$  value of their respective bottom envelopes. **D** Heatmap of gene expression levels for TGF- $\beta$  signaling pathway-related genes in A549 cells overexpressing NOVA2. Green, black, and red shading represent low, intermediate, and high gene expression, respectively. **E** qPCR analysis of selected genes from TGF- $\beta$  signaling pathway in A549 cells overexpressing NOVA2. **F**, **G** A549 (**F**) and H1975 (**G**) cells stably overexpressing NOVA2 were serum-starved for 24 h, then treated with or without TGF- $\beta$ 1 (5 ng/ml) for 24 h. Immunoblotting was performed to determine protein levels of NOVA2, SMAD3, and p-SMAD3.  $\beta$ -actin served as an internal control. **H**, **I** NOVA2-silenced A549 (**H**) and H1975 (**I**) cells were treated as described above. Immunoblotting analysis was conducted to assess the protein levels of NOVA2, SMAD3, and p-SMAD3.  $\beta$ -actin was used as an internal control. **J** NOVA2-overexpressing A549 and H1975 cells were treated as described and subjected to qRT-PCR for determining the mRNA expression of downstream genes in TGF- $\beta$ /SMAD signaling pathway, including *PAI-1*, *Slug*, *Snail*, *CDH1*, and *CDH2*. Data are presented as the mean  $\pm$  SD of  $n = 3$  biological replicates. \* $P < 0.05$ , \*\* $P < 0.01$ , \*\*\* $P < 0.001$  by unpaired Student's  $t$  test.

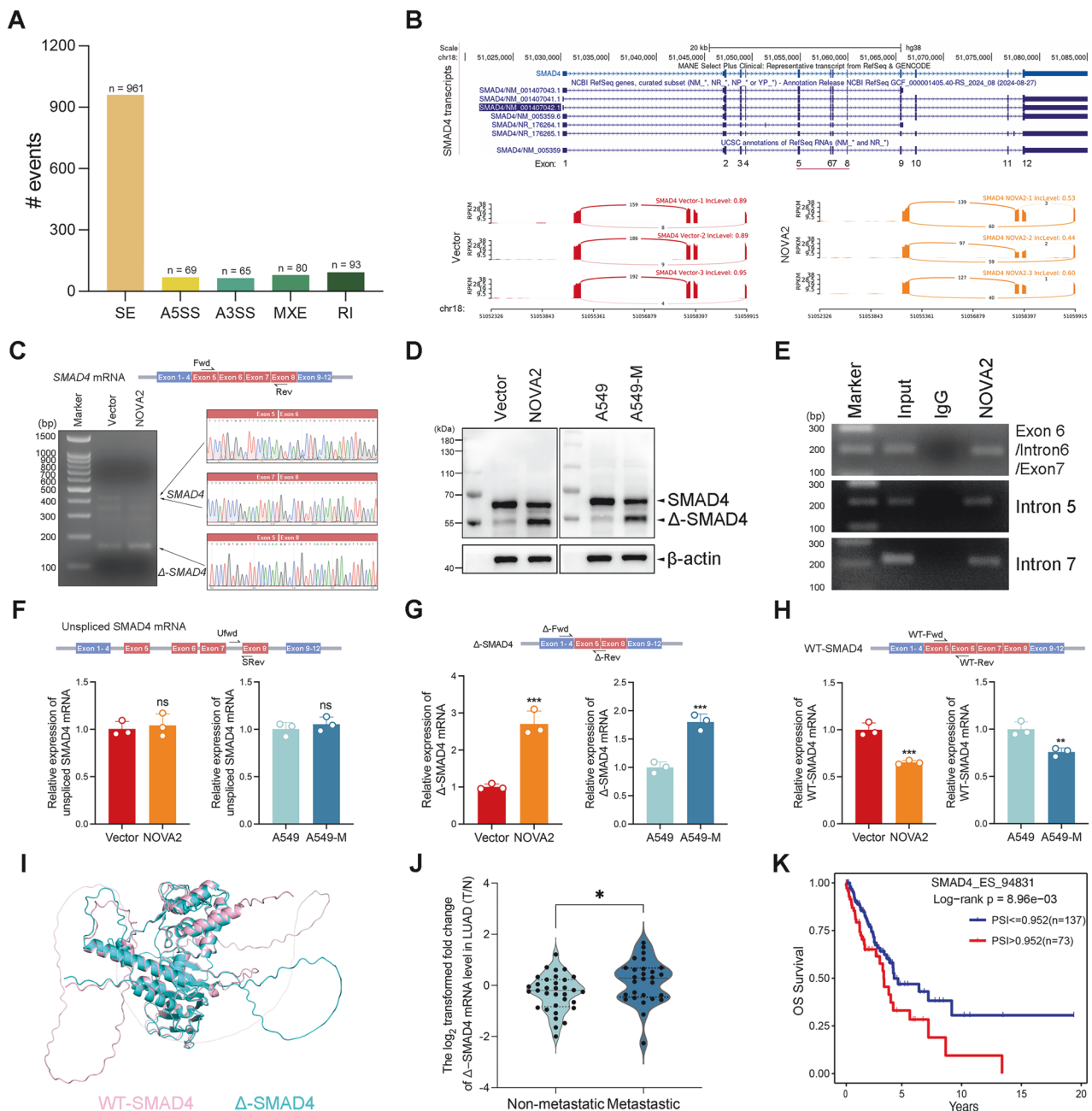
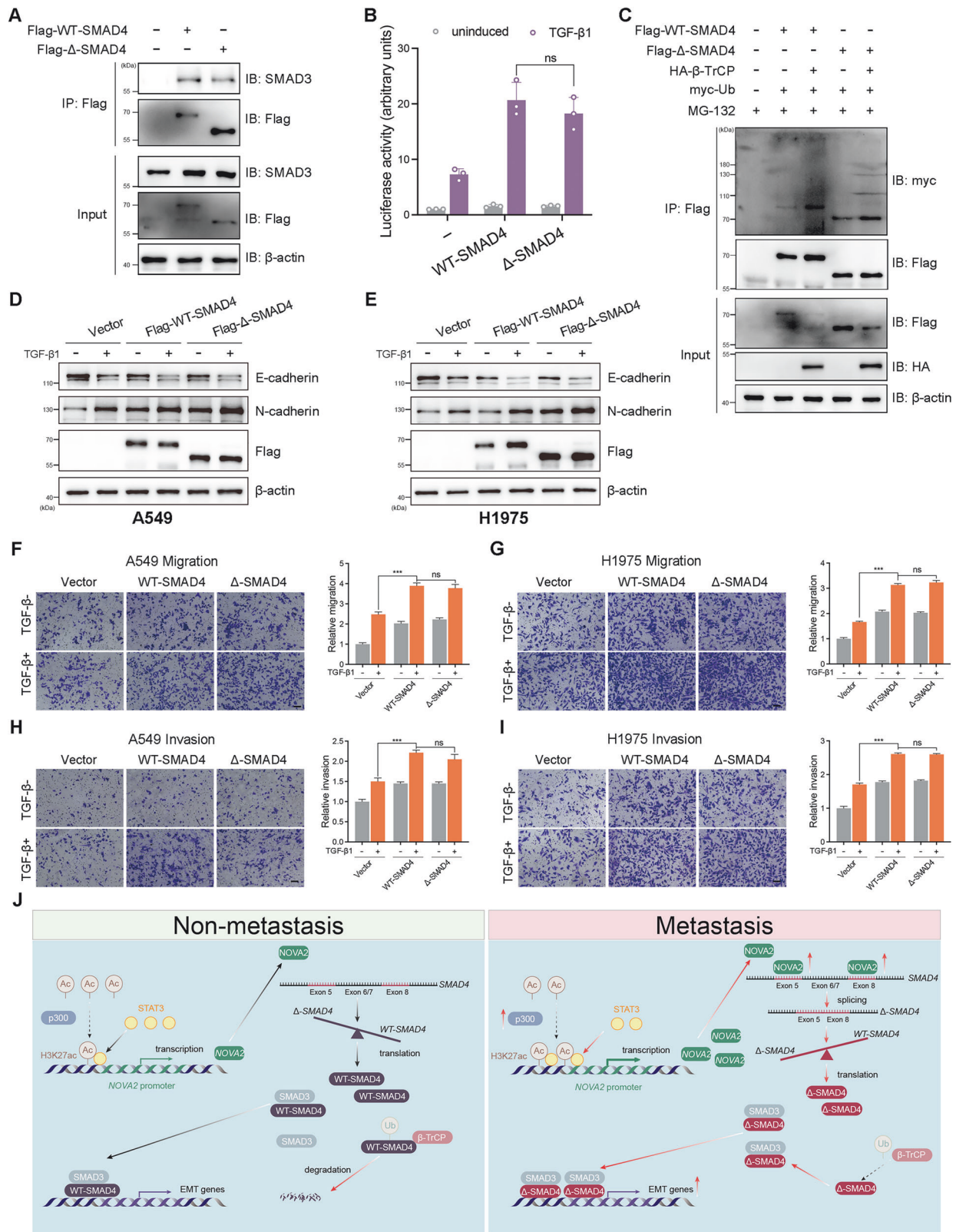


**Fig. 6** NOVA2 regulates SMAD4 mRNA splicing in LUAD cells. **A** Summary of significant alternative splicing events observed upon NOVA2 overexpression in A549 cells, detected by rMATS. SE, skipped exon; A5SS, alternative 5' splice site; A3SS, alternative 3' splice site; MXE, mutually exclusive exons; RI, retained intron. **B** Representative sashimi plot showing RNA-seq read coverage across the SMAD4 gene. SMAD4 isoforms are presented at the top. Arcs correspond to reads spanning exon-exon junctions, with the number of reads for each junction are indicated below. **C** DNA electrophoresis of two SMAD4 isoforms detected by PCR from NOVA2-overexpressing A549 cells (Left panel). Sanger sequencing results of two PCR bands, showing differences at exon 6/exon 7 (Right panel). **D** Protein abundance of WT-SMAD4 and  $\Delta$ -SMAD4 in A549 cells stably overexpressing NOVA2 and A549-M cells. **E** RT-PCR analysis of RIP results using an anti-NOVA2 antibody, testing for Exon 6/Intron 6/Exon 7, Intron 5, and Intron 7 regions. **F** qRT-PCR analysis of unspliced SMAD4 transcripts in A549 cells overexpressing NOVA2 and A549-M cells. Top: PCR primer locations. Data are presented as the mean  $\pm$  SD of  $n = 3$  biological replicates. ns, not significant by unpaired Student's  $t$  test. **G**, **H** qRT-PCR analysis of  $\Delta$ -SMAD4 (G) and WT-SMAD4 (H) transcripts in A549 cells overexpressing NOVA2 and A549-M cells. Top: PCR primer locations. Data are presented as the mean  $\pm$  SD of  $n = 3$  biological replicates. \*\*\* $P < 0.001$  by unpaired Student's  $t$  test. **I** Structural superposition of WT-SMAD4 (pink) and  $\Delta$ -SMAD4 (cyan). **J** qRT-PCR analysis of  $\Delta$ -SMAD4 mRNA expression in 61 LUAD tissues and matched paracarcinoma tissues. The Y-axis represents the fold change in  $\Delta$ -SMAD4 mRNA expression (T/N) in LUAD tissues (T) and paracarcinoma tissues (N). Data are presented as the mean  $\pm$  SD of  $n = 3$  biological replicates. \* $P < 0.05$  by unpaired Student's  $t$  test. **K** Survival curve analysis was conducted to assess the influence of SMAD4\_ES\_94832 (exon 6 and exon 7 skipping in SMAD4) using the OncoSplicing database. PSI percent spliced in.



introns (Fig. 6E), suggesting a potential involvement of NOVA2 in regulating SMAD4 transcript splicing efficiency. In fact, quantification of unspliced SMAD4 transcripts spanning the intron 7-exon 8 junctions showed no significant change in A549-overexpressing NOVA2 and A549-M cells, implying that NOVA2 does not enhance

SMAD4 splicing efficiency (Fig. 6F). However, in A549 cells overexpressing NOVA2 and A549-M cells, Δ-SMAD4 mRNA expression was upregulated (Fig. 6G) while WT-SMAD4 mRNA expression was downregulated (Fig. 6H). These observations prompted an exploration of the molecular mechanisms



**Fig. 7**  $\beta$ -TrCP-mediated  $\Delta$ -SMAD4 ubiquitination is diminished and  $\Delta$ -SMAD4 facilitates TGF- $\beta$ -induced EMT and invasion of LUAD cells. **A** 293 T cells transfected with Flag-tagged WT-SMAD4 or Flag-tagged  $\Delta$ -SMAD4 (generated from A549-M cells) were subjected to co-IP analysis. Flag-tagged WT-SMAD4 and Flag-tagged  $\Delta$ -SMAD4 proteins were immunoprecipitated using anti-Flag antibodies. Binding of WT-SMAD4 or  $\Delta$ -SMAD4 to SMAD3 was detected by immunoblotting with an anti-FLAG antibody. **B** In the presence or absence of TGF- $\beta$ 1, luciferase activity of the *PAL-1* promoter was determined in A549 cells transfected with Flag-tagged WT-SMAD4 or Flag-tagged  $\Delta$ -SMAD4. Data are presented as the mean  $\pm$  SD of  $n = 3$  biological replicates. ns, not significant by unpaired Student's *t* test. **C** Flag-tagged WT-SMAD4, Flag-tagged  $\Delta$ -SMAD4, HA-tagged  $\beta$ -TrCP, and/or myc-tagged Ub vectors were co-transfected into 293 T cells as indicated for 48 h. Cell lysates were then immunoprecipitated with anti-Flag antibodies and immunoblotted with antibodies against Flag or myc. Total lysates were immunoblotted with the indicated antibodies, and  $\beta$ -actin served as a loading control. **D, E** After serum starvation for 24 h, WT-SMAD4 or  $\Delta$ -SMAD4 overexpressed A549 (D) and H1975 (E) cells were treated with or without TGF- $\beta$ 1 (5 ng/ml) for 24 h. The expression of EMT markers (N-cadherin and E-cadherin) was determined using immunoblotting.  $\beta$ -actin was used as an internal control. **F–I** In the presence or absence of TGF- $\beta$ 1, the migratory and invasive capabilities of A549 and H1975 cells overexpressing WT-SMAD4 and  $\Delta$ -SMAD4 were evaluated by Transwell assays as described in Fig. 2B, C. Migrated and invasive cells were stained and counted under a light microscope. Scale bar, 100  $\mu$ m. Data are presented as the mean  $\pm$  SD of  $n = 5$  biological replicates. ns, not significant; \*\*\* $P < 0.001$  by unpaired Student's *t* test. **J** Schematic mechanism model: In non-metastatic LUAD, low p300 expression reduces H3K27ac enrichment at the *NOVA2* promoter, maintaining low *NOVA2* expression. Consequently, E3 ubiquitin ligase  $\beta$ -TrCP interacts with WT-SMAD4 to degrade normal SMAD4 levels (left panel). In metastatic LUAD, high p300 expression increases H3K27ac enrichment at the *NOVA2* promoter, enhancing STAT3 binding and thereby strengthening *NOVA2* transcription, and increased *NOVA2* promotes  $\Delta$ -SMAD4 isoform formation that evades  $\beta$ -TrCP-mediated ubiquitination, eventually potentiates TGF- $\beta$ -induced EMT to facilitate LUAD metastasis (right panel).

underlying the exclusion of exon 6–7 during SMAD4 splicing. Since the deletion of exon 6–7 occurs within the middle linker region of SMAD4, it was deduced that this deletion would not affect the protein's translation efficiency. To explore the functional consequences of this deletion, AlphaFold3 was employed to simulate the structures of wild-type and  $\Delta$ -SMAD4, indicating that the deletion does not disrupt the overall architecture of MH1 and MH2 domains (Fig. 6I).

Based on the fact that SMAD4 is a key effector in TGF- $\beta$  signaling cascade and our findings that *NOVA2* is implicated in TGF- $\beta$  signaling, we investigated the functional consequences of  $\Delta$ -SMAD4 expression. Immunoprecipitation assays showed that  $\Delta$ -SMAD4 forms a stable complex with SMAD3, mimicking the SMAD3/SMAD4 interaction observed in the canonical TGF- $\beta$ /SMAD signaling (Fig. 7A). Furthermore, overexpression of  $\Delta$ -SMAD4 induced similar activation of SMAD-mediated *PAL-1* promoter reporter gene in A549 cells with TGF- $\beta$ 1 stimulation (Fig. 7B). Demagney *et al.* have demonstrated that T277 phosphorylation is required for SMAD4 degradation by E3 ubiquitin ligase  $\beta$ -TrCP [38]. Thus, we hypothesized that the deletion of amino acids 223–302 of SMAD4 ( $\Delta$ -SMAD4) (Fig. 6C, D) may confer resistance to degradation by  $\beta$ -TrCP. Co-immunoprecipitation analysis indicated that  $\beta$ -TrCP-mediated ubiquitination level of  $\Delta$ -SMAD4 was lower than that of WT-SMAD4 (Fig. 7C). Furthermore, like WT-SMAD4,  $\Delta$ -SMAD4 promoted TGF- $\beta$ -induced EMT and migration and invasion of A549 and H1975 cells (Fig. 7D–I), suggesting that  $\Delta$ -SMAD4 served the same function as WT-SMAD4. Subsequently, we knocked down WT-SMAD4 or  $\Delta$ -SMAD4 in *NOVA2*-overexpressing A549 and H1975 cells (Fig. 55A) and found that on TGF- $\beta$  treatment,  $\Delta$ -SMAD4 knockdown had a stronger inhibitory effect on the upregulation of N-cadherin and Snail than did WT-SMAD4 knockdown. The downregulation of E-cadherin was weakly rescued by WT-SMAD4 knockdown, whereas  $\Delta$ -SMAD4 knockdown largely abrogated this downregulation (Fig. 55B). Upon TGF- $\beta$  stimulation, cells with  $\Delta$ -SMAD4 knockdown showed lower migration and invasion than those with WT-SMAD4 knockdown (Fig. 55C–55F). Clinically,  $\Delta$ -SMAD4 expression was significantly higher in metastatic LUAD patients compared to that in non-metastatic patients (Fig. 6J and Table S1). Survival analysis from the OncoSplicing database showed that LUAD individuals with lower PSI (Percent Spliced In) of  $\Delta$ -SMAD4 exhibited superior overall survival compared to those with higher PSI (Fig. 6K) [39]. Collectively, these results suggest that *NOVA2*-mediated splicing of SMAD4 to  $\Delta$ -SMAD4 leads to the loss of critical degron motifs, diminishing  $\Delta$ -SMAD4 ubiquitination by  $\beta$ -TrCP and facilitating TGF- $\beta$ -induced EMT and invasion of LUAD cells.

### **NOVA2 facilitates TGF- $\beta$ -induced EMT and invasion of LUAD cells in a $\Delta$ -SMAD4-dependent manner**

Next, we tested whether *NOVA2* potentiates TGF- $\beta$ -driven metastatic progression. *NOVA2*-overexpressing A549 and H1975 cell lines were subjected to TGF- $\beta$ 1 stimulation (5 ng/ml, 24 h). Immunoblotting revealed significantly increased expression of mesenchymal markers (N-cadherin, Snail) or decreased expression of epithelial marker E-cadherin in LUAD cells overexpressing *NOVA2* (Fig. S6A). Immunofluorescence staining of F-actin showed that TGF- $\beta$ 1 induced a spindle-shaped mesenchymal morphology in control cells, while *NOVA2*-overexpressing A549 and H1975 cells displayed further morphological polarization, indicative of enhanced EMT (Fig. S6B). Moreover, *NOVA2* overexpression significantly enhanced TGF- $\beta$ 1-induced migratory and invasive capacities (Fig. S6C and S6D). In contrast, *NOVA2* silencing attenuated TGF- $\beta$ 1-induced EMT, as indicated by upregulation of E-cadherin and downregulation of N-cadherin and Snail (Fig. S6E and S6F), and *NOVA2* silencing inhibited TGF- $\beta$ 1-induced migration and invasion of LUAD cells (Fig. S6G and S6H), highlighting that *NOVA2* expression promotes TGF- $\beta$ -driven migration and invasion.

Our aforementioned findings indicate that *NOVA2* drives SMAD4 AS and enhances TGF- $\beta$ -induced EMT and invasion in LUAD cells. To assess whether these effects are dependent on the truncated  $\Delta$ -SMAD4 isoform, rescue experiments were performed in *NOVA2*-overexpressing A549 and H1975 cells. Isoform-specific siRNAs-mediated knockdown of  $\Delta$ -SMAD4 significantly attenuated *NOVA2*-driven upregulation of  $\Delta$ -SMAD4 expression (Fig. S7A).  $\Delta$ -SMAD4 knockdown diminished the impact of *NOVA2* overexpression on EMT-related proteins in LUAD cells, as indicated by downregulation of N-cadherin and Snail (Fig. S7B). Moreover,  $\Delta$ -SMAD4 knockdown completely abolished TGF- $\beta$ -induced cell migration and invasion in *NOVA2*-overexpressing A549 and H1975 cells (Fig. S7C and S7D). These findings provide compelling evidence that *NOVA2*-driven SMAD4 AS is an important mechanism by which *NOVA2* facilitates TGF- $\beta$ -induced EMT.

### **DISCUSSION**

RBP's play key roles in various biological processes, and their deregulation is increasingly recognized as a significant factor in cancer progression [40]. Growing evidence highlights RBPs as key drivers of tumor metastasis, positioning them as promising diagnostic and prognostic biomarkers [13]. Lung cancer, the leading cause of cancer-related death, underscores the need for improved predictive biomarkers to ensure that patients receive the most effective treatments. To identify an RBP signature for

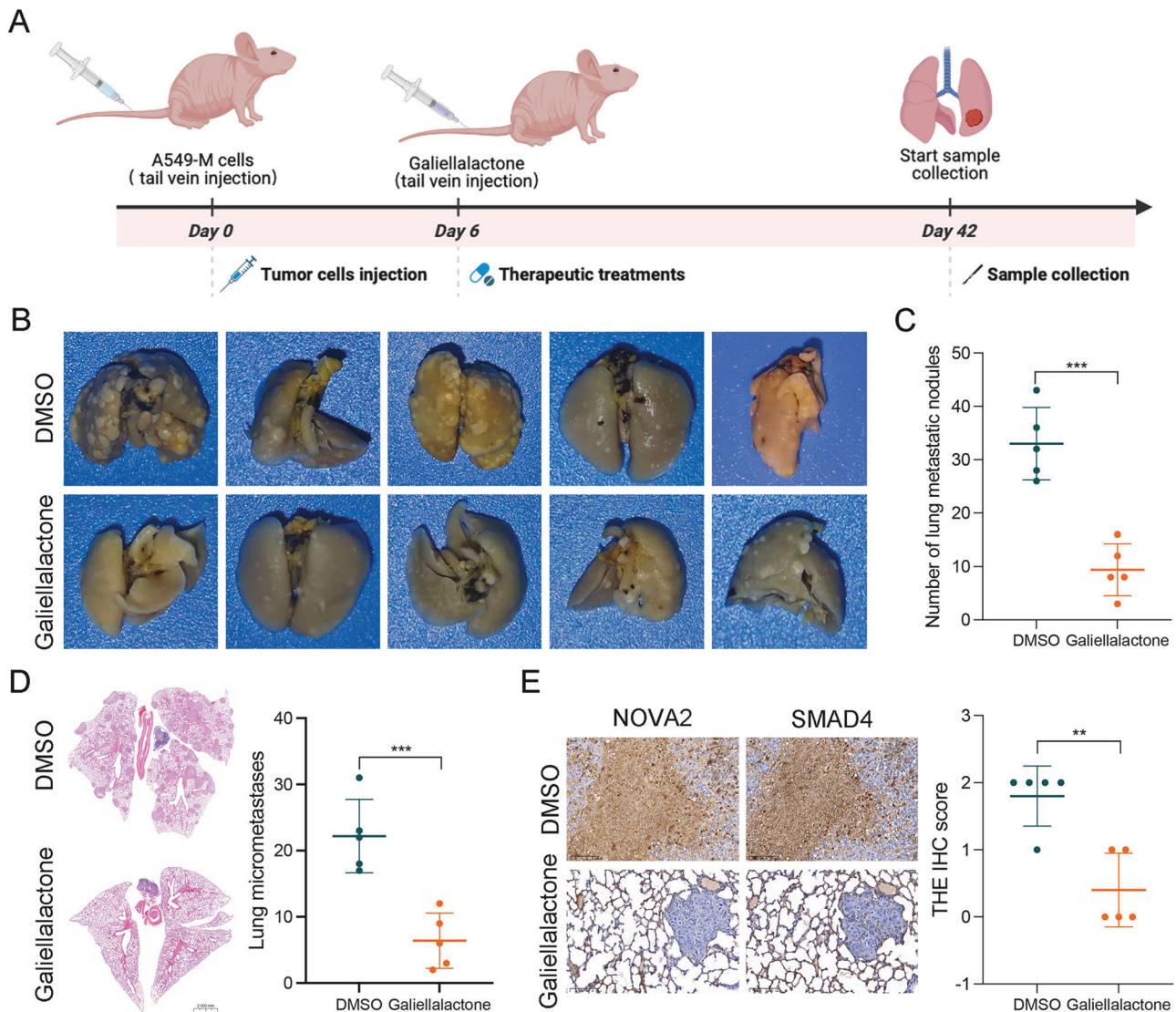


**Fig. 8** STAT3 inhibitor galiellalactone attenuates lung metastasis and NOVA2/SMAD4 expression in a murine model of A549-M cell metastasis. **A** Schematic flowchart of Galiellalactone treatment in the in vivo metastasis model. A549-M cells with elevated NOVA2 expression (Fig. 1C) were intravenously injected into BALB/c nude mice to establish metastatic tumor models (5 mice per group). Starting from Day 6, Galiellalactone (1 mg/kg) was administered via tail vein injection once daily. Samples were collected on Day 42 for subsequent downstream analyses. **B**, **C** Representative images of metastatic lung nodules (**B**) and the number of metastatic nodules was compared between the Galiellalactone treatment and control groups (**C**). Lungs were surgically resected and stained as described in “Materials and Methods”. Data are shown as the mean  $\pm$  SD of  $n = 5$  biological replicates. \*\*\* $P < 0.001$  by unpaired Student’s  $t$  test. **D** Representative images of H&E-stained lung tumors (Left panel) and quantification of micrometastases counts in lung tissues from the Galiellalactone treatment and control groups (Right panel). Data are shown as the mean  $\pm$  SD of  $n = 5$  biological replicates. \*\*\* $P < 0.001$  by unpaired Student’s  $t$  test. **E** Representative IHC images and IHC scores for NOVA2 and SMAD4 expression in lung metastases from the Galiellalactone treatment and control groups. Staining intensity was scored as 0 (weak), 1 (moderate), and 2 (strong). Data are shown as the mean  $\pm$  SD of  $n = 5$  biological replicates. \*\* $P < 0.01$  by unpaired Student’s  $t$  test.

LUAD metastasis, computational algorithms were employed across different metastatic LUAD cohorts and the RBP database, followed by validation of NOVA2 expression in our highly metastatic cell line [35]. Functional data demonstrated that NOVA2 functions as an oncogenic RBP in metastatic LUAD cells. Mechanistically, p300 elevates H3K27ac levels at the NOVA2 promoter, thereby promoting STAT3-dependent transcriptional activation. NOVA2 is involved TGF- $\beta$  signaling pathway and mediates SMAD4 splicing to form an isoform that avoids degradation, leading to LUAD metastasis (Fig. 7J).

Lysine acetylation dynamically regulates chromatin accessibility and transcriptional activation, with acetylation being deposited by lysine acetyltransferases, removed by deacetylases, and

recognized by bromodomains or YEATS domains, forming an integrated “write-erase-read” epigenetic network [41]. By catalyzing histone acetylation, p300 functions as a transcriptional co-activator, facilitating gene transcription [42]. Previous studies have highlighted the role of histone H3K27ac in promoting cancer progression in human cancers, including colon, lung, and breast cancers [43–46]. However, the TFs that regulate the expression of RBPs remain underexplored. In this study, our detailed molecular analyses revealed that p300-mediated H3K27ac enhances STAT3-dependent transcriptional activation of NOVA2 (Figs. 3, 4). Although the upregulation of p300 has been found in LUAD tissues [47], further studies are warranted to elucidate the reason why p300 expression is aberrant in metastasis LUAD. STAT3, a TF

critical to oncogenesis, regulates genes involved in cell survival, proliferation, invasion, and metastasis [48, 49]. Gene expression regulation occurs at the chromatin, transcriptional, or post-transcriptional levels, mediated by epigenetic factors (such as chromatin-regulating factors and non-coding RNAs), TFs, and microRNAs. Understanding NOVA2 regulation offers an opportunity to integrate cancer metastasis with epigenetic mechanisms. Most studies on NOVA2 regulation have focused on non-coding RNAs [50–52]. Our data uncover a novel mechanism underlying the upregulation of NOVA2 in metastatic cancer cells.

Splicing dysregulation events can serve as molecular markers of cancer, and in some cases, they may be directly responsible for tumorigenesis [53]. Thus, a mechanistic study of splicing dysregulation offers valuable insights into cancer progression [14]. This study exemplifies how RBPs mediate splicing to control critical AS events in cancer. Moreover, depletion of NOVA2 has been shown to inhibit tumor metastasis in both cell culture systems and mouse models, suggesting that targeting NOVA2 activity could provide a promising therapeutic approach. Additionally, other NOVA2-regulated events may contribute to tumor pathogenesis and progression. For instance, dysregulation of NOVA2-mediated AS has been linked to tumor angiogenesis and cancer progression [19, 20, 54]. These findings indicate that NOVA2 mediates multiple AS events that are critical to cancer progression.

Our results reveal a distinct difference in the expression levels of the active splice variant of  $\Delta$ -SMAD4 between primary and metastatic tumors (Fig. 6G, J). Although SMAD4 transcripts with or without exon 6–7 inclusion exhibit similar stabilities, the exon 6–7-skipped splice variant shows higher protein expression. This suggests that skipping this exon results in the production of a more stable protein. This observation raises an important question: To what extent do AS events contribute to the expression of stable protein products? Recent structural modeling of splice variants from genes in the 1% of the genome surveyed by the ENCODE Consortium predicts that many AS events likely disrupt correct protein folding, as the alternatively spliced regions often interfere with core structural domains [55]. However, our findings contrast with this, as exon 6–7 skipping in SMAD4 does not appear to dramatically alter its structure or function (Fig. 6I). Our results are consistent with the notion that spliced SMAD4 variants can interact with activated R-SMADs, form transcriptional complexes, and activate TGF- $\beta$ /SMAD signaling [56]. Additionally, even a relatively small change in transcript abundance has been shown to be sufficient to trigger oncogenic effects in cells [19, 57, 58]. Notably, our data suggest that high NOVA2 expression in metastatic LUAD promotes exon 6–7 skipping of SMAD4. This implies that NOVA2 post-translationally regulates SMAD4 by preventing its ubiquitin-mediated degradation. Consequently, NOVA2 can activate TGF- $\beta$ /SMAD signaling pathway in LUAD cells, promoting their metastatic potential.

Although our findings highlight that the STAT3-NOVA2 axis serves as an upstream regulator of  $\Delta$ -SMAD4 during LUAD metastasis, it is not yet fully validated in vivo. Thereupon, we established a lung metastasis model by injecting A549-M cells with elevated NOVA2 expression, BALB/c nude mice were then treated with an STAT3 inhibitor Galiellalactone (disrupting the interaction between STAT3 and its target genes) (Fig. 8A). The mice injected with Galiellalactone developed significantly fewer metastatic nodules and micrometastases (Fig. 8B–D) and showed markedly decreased NOVA2 and SMAD4 expression (Fig. 8E).

Our current findings suggest that NOVA2 promotes LUAD metastasis by splicing SMAD4. However, a key limitation of the present study is that NOVA2-regulated splicing events beyond SMAD4 likely contribute to LUAD metastasis. For example, an additional candidate NOVA2-targeted splicing gene FN1, which was identified in our RNA-seq dataset (Table S3), needs to be validated in LUAD metastasis.

In summary, our findings identify a novel mechanism by which STAT3-mediated transcriptional upregulation of NOVA2 promotes SMAD4 splicing in metastatic LUAD, and suggest that the STAT3-NOVA2- $\Delta$ -SMAD4 axis drives EMT and LUAD metastasis, which may be a promising therapeutic target for treating LUAD.

## DATA AVAILABILITY

The data generated in Fig. 1A are retrieved from EuRBPDB [26], ATTRACT [27], CancerSEA [28], and prognostic gene signatures [29] online databases. The gene expression correlation analyzed in Fig. 4F, S3E and S3F are available from GEPIA database (<http://gepia.cancer-pku.cn/>). The RNA-seq data generated in Figs. 5A and 6A are included in supplementary materials, and all other raw data are available upon request from the corresponding author.

## REFERENCES

- Chaffer CL, Weinberg RA. A perspective on cancer cell metastasis. *Science*. 2011;331:1559–64.
- Brandt WS, Yan W, Zhou J, Tan KS, Montecalvo J, Park BJ, et al. Outcomes after neoadjuvant or adjuvant chemotherapy for cT2-4N0-1 non-small cell lung cancer: A propensity-matched analysis. *J Thorac Cardiovasc Surg*. 2019;157:743–753.e743.
- Lou F, Huang J, Sima CS, Dycoco J, Rusch V, Bach PB. Patterns of recurrence and second primary lung cancer in early-stage lung cancer survivors followed with routine computed tomography surveillance. *J Thorac Cardiovasc Surg*. 2013;145:75–81.
- Esposito M, Ganesan S, Kang Y. Emerging strategies for treating metastasis. *Nat Cancer*. 2021;2:258–70.
- Watanabe K, Tsuboi M, Sakamaki K, Nishii T, Yamamoto T, Nagashima T, et al. Postoperative follow-up strategy based on recurrence dynamics for non-small-cell lung cancer. *Eur J Cardiothorac Surg*. 2016;49:1624–31.
- Cancer Genome Atlas Research Network. Comprehensive molecular profiling of lung adenocarcinoma. *Nature*. 2014;511:543–50.
- Sterne-Weiler T, Sanford JR. Exon identity crisis: disease-causing mutations that disrupt the splicing code. *Genome Biol*. 2014;15:201.
- Yang X, Coulombe-Huntington J, Kang S, Sheynkman GM, Hao T, Richardson A, et al. Widespread expansion of protein interaction capabilities by alternative splicing. *Cell*. 2016;164:805–17.
- Chabot B, Shkreta L. Defective control of pre-messenger RNA splicing in human disease. *J Cell Biol*. 2016;212:13–27.
- Lee SC, Abdel-Wahab O. Therapeutic targeting of splicing in cancer. *Nat Med*. 2016;22:976–86.
- Lu ZX, Huang Q, Park JW, Shen S, Lin L, Tokheim CJ, et al. Transcriptome-wide landscape of pre-mRNA alternative splicing associated with metastatic colonization. *Mol Cancer Res*. 2015;13:305–18.
- Trincado JL, Sebestyen E, Pages A, Eyras E. The prognostic potential of alternative transcript isoforms across human tumors. *Genome Med*. 2016;8:85.
- Wang S, Sun Z, Lei Z, Zhang HT. RNA-binding proteins and cancer metastasis. *Semin Cancer Biol*. 2022;86:748–68.
- Wang Y, Chen D, Qian H, Tsai YS, Shao S, Liu Q, et al. The splicing factor RBM4 controls apoptosis, proliferation, and migration to suppress tumor progression. *Cancer Cell*. 2014;26:374–89.
- Oltean S, Bates DO. Hallmarks of alternative splicing in cancer. *Oncogene*. 2014;33:5311–8.
- Buckanovich RJ, Yang YY, Darnell RB. The onconeural antigen Nova-1 is a neuron-specific RNA-binding protein, the activity of which is inhibited by paraneoplastic antibodies. *J Neurosci*. 1996;16:1114–22.
- Meldolesi J. Alternative Splicing by NOVA Factors: From Gene Expression to Cell Physiology and Pathology. *Int J Mol Sci*. 2020;21:3941.
- Campos-Melo D, Droppelmann CA, Volkner K, Strong MJ. RNA-binding proteins as molecular links between cancer and neurodegeneration. *Biogerontology*. 2014;15:587–610.
- Pradella D, Defforian G, Pezzotta A, Di Matteo A, Belloni E, Campolungo D, et al. A ligand-insensitive UNC5B splicing isoform regulates angiogenesis by promoting apoptosis. *Nat Commun*. 2021;12:4872.
- Meldolesi F, Belloni E, Giordano M, Campioni M, Forneris F, Paronetto MP, et al. A novel L1CAM isoform with angiogenic activity generated by NOVA2-mediated alternative splicing. *Elife*. 2019;8:e44305.
- Cui W, Fowles DJ, Bryson S, Duffie E, Ireland H, Balmain A, et al. TGF $\beta$ 1 inhibits the formation of benign skin tumors, but enhances progression to invasive spindle carcinomas in transgenic mice. *Cell*. 1996;86:531–42.
- David CJ, Massague J. Contextual determinants of TGF $\beta$  action in development, immunity and cancer. *Nat Rev Mol Cell Biol*. 2018;19:419–35.



23. Katsuno Y, Lamouille S, Derynck R. TGF- $\beta$  signaling and epithelial-mesenchymal transition in cancer progression. *Curr Opin Oncol*. 2013;25:76–84.
24. Massague J, Seoane J, Wotton D. Smad transcription factors. *Genes Dev*. 2005;19:2783–810.
25. Xu P, Lin X, Feng XH. Posttranslational Regulation of Smads. *Cold Spring Harb Perspect Biol*. 2016;8:a022087.
26. Liao JY, Yang B, Zhang YC, Wang XJ, Ye Y, Peng JW, et al. EuRBPDB: a comprehensive resource for annotation, functional and oncological investigation of eukaryotic RNA binding proteins (RBPs). *Nucleic Acids Res*. 2020;48:D307–D313.
27. Giudice G, Sanchez-Cabo F, Torroja C, Lara-Pezzi E. ATTRACT-a database of RNA-binding proteins and associated motifs. *Database (Oxford)*. 2016;2016:baw035.
28. Yuan H, Yan M, Zhang G, Liu W, Deng C, Liao G, et al. CancerSEA: a cancer single-cell state atlas. *Nucleic Acids Res*. 2019;47:D900–D908.
29. Zhang Y, Fu F, Zhang Q, Li L, Liu H, Deng C, et al. Evolutionary proteogenomic landscape from pre-invasive to invasive lung adenocarcinoma. *Cell Rep Med*. 2024;5:101358.
30. Jorgensen HF, Azuara V, Amois S, Spivakov M, Terry A, Nesterova T, et al. The impact of chromatin modifiers on the timing of locus replication in mouse embryonic stem cells. *Genome Biol*. 2007;8:R169.
31. Song M, Yang X, Ren X, Maliskova L, Li B, Jones IR, et al. Mapping cis-regulatory chromatin contacts in neural cells links neuropsychiatric disorder risk variants to target genes. *Nat Genet*. 2019;51:1252–62.
32. Mortimer SA, Kidwell MA, Doudna JA. Insights into RNA structure and function from genome-wide studies. *Nat Rev Genet*. 2014;15:469–79.
33. Castel SE, Martienssen RA. RNA interference in the nucleus: roles for small RNAs in transcription, epigenetics and beyond. *Nat Rev Genet*. 2013;14:100–12.
34. Fiszbain A, Krick KS, Begg BE, Burge CB. Exon-mediated activation of transcription starts. *Cell*. 2019;179:1551–65.e1517.
35. Wang Z, Lei Z, Wang Y, Wang S, Wang JP, Jin E, et al. Bone-metastatic lung adenocarcinoma cells bearing CD74-ROS1 fusion interact with macrophages to promote their dissemination. *Oncogene*. 2024;43:2215–27.
36. Cai L, Sutter BM, Li B, Tu BP. Acetyl-CoA induces cell growth and proliferation by promoting the acetylation of histones at growth genes. *Mol Cell*. 2011;42:426–37.
37. Yang YY, Yin GL, Darnell RB. The neuronal RNA-binding protein Nova-2 is implicated as the autoantigen targeted in POMA patients with dementia. *Proc Natl Acad Sci USA*. 1998;95:13254–9.
38. Demagny H, Araki T, De Robertis EM. The tumor suppressor Smad4/DPC4 is regulated by phosphorylations that integrate FGF, Wnt, and TGF- $\beta$  signaling. *Cell Rep*. 2014;9:688–700.
39. Zhang Y, Liu K, Xu Z, Li B, Wu X, Fan R, et al. OncoSplicing 3.0: an updated database for identifying RBPs regulating alternative splicing events in cancers. *Nucleic Acids Res*. 2025;53:D1460–D1466.
40. Gerstberger S, Hafner M, Tuschl T. A census of human RNA-binding proteins. *Nat Rev Genet*. 2014;15:829–45.
41. Zhou MM, Cole PA. Targeting lysine acetylation readers and writers. *Nat Rev Drug Discov*. 2025;24:112–33.
42. Rice JC, Allis CD. Histone methylation versus histone acetylation: new insights into epigenetic regulation. *Curr Opin Cell Biol*. 2001;13:263–73.
43. Liu D, Zhang H, Cong J, Cui M, Ma M, Zhang F, et al. H3K27 acetylation-induced lncRNA EIF3J-AS1 improved proliferation and impeded apoptosis of colorectal cancer through miR-3163/YAP1 axis. *J Cell Biochem*. 2020;121:1923–33.
44. Zhang Y, Liu Z, Yang X, Lu W, Chen Y, Lin Y, et al. Erratum: H3K27 acetylation activated-COL6A1 promotes osteosarcoma lung metastasis by repressing STAT1 and activating pulmonary cancer-associated fibroblasts: Erratum. *Theranostics*. 2022;12:4604–5.
45. Ye P, Lv X, Aizemaiti R, Cheng J, Xia P, Di M. H3K27ac-activated LINC00519 promotes lung squamous cell carcinoma progression by targeting miR-450b-5p/miR-515-5p/YAP1 axis. *Cell Prolif*. 2020;53:e12797.
46. Han M, Qian X, Cao H, Wang F, Li X, Han N, et al. lncRNA ZNF649-AS1 Induces Trastuzumab Resistance by Promoting ATG5 Expression and Autophagy. *Mol Ther*. 2020;28:2488–502.
47. Wang YC, Wu YS, Hung CY, Wang SA, Young MJ, Hsu TI, et al. USP24 induces IL-6 in tumor-associated microenvironment by stabilizing p300 and beta-TrCP and promotes cancer malignancy. *Nat Commun*. 2018;9:3996.
48. Frank DA. Transcription factor STAT3 as a prognostic marker and therapeutic target in cancer. *J Clin Oncol*. 2013;31:4560–1.
49. Bai L, Zhou H, Xu R, Zhao Y, Chinnaswamy K, McEachern D, et al. A Potent and Selective Small-Molecule Degradator of STAT3 Achieves Complete Tumor Regression In Vivo. *Cancer Cell*. 2019;36:498–511.e417.
50. Liu J, Yu Q, Yang X. Circ\_0102231 inactivates the PI3K/AKT signaling pathway by regulating the miR-635/NOVA2 pathway to promote the progression of non-small cell lung cancer. *Thorac Cancer*. 2023;14:3453–64.
51. Xia F, Xie M, He J, Cheng D. Circ\_0004140 promotes lung adenocarcinoma progression by upregulating NOVA2 via sponging miR-330-5p. *Thorac Cancer*. 2023;14:3483–94.
52. Dhara C, Dhara A, Gantayat S. A Robust NSCLC Biomarker- Mir-7-5p: Its in-silico validation and potential SPR-based probe for detection. *Microna*. 2025;14:112–23.
53. David CJ, Manley JL. Alternative pre-mRNA splicing regulation in cancer: pathways and programs unhinged. *Genes Dev*. 2010;24:2343–64.
54. Di Matteo A, Belloni E, Pradella D, Chiaravalli AM, Pini GM, Bugatti M, et al. Alternative splicing changes promoted by NOVA2 upregulation in endothelial cells and relevance for gastric cancer. *Int J Mol Sci*. 2023;24:8102.
55. Tress ML, Martelli PL, Frankish A, Reeves GA, Wesselink JJ, Yeats C, et al. The implications of alternative splicing in the ENCODE protein complement. *Proc Natl Acad Sci USA*. 2007;104:5495–5500.
56. Pierreux CE, Nicolas FJ, Hill CS. Transforming growth factor beta-independent shuttling of Smad4 between the cytoplasm and nucleus. *Mol Cell Biol*. 2000;20:9041–54.
57. Zhao C, Zhao JW, Zhang YH, Zhu YD, Yang ZY, Liu SL, et al. PTBP3 mediates IL-18 exon skipping to promote immune escape in gallbladder cancer. *Adv Sci (Weinh)*. 2024;11:e2406633.
58. DaSilva JO, Yang K, Perez Bay AE, Andreev J, Ngoi P, Pyles E, et al. A biparatopic antibody that modulates MET trafficking exhibits enhanced efficacy compared with parental antibodies in MET-driven tumor models. *Clin Cancer Res*. 2020;26:1408–19.

## ACKNOWLEDGEMENTS

We are grateful for the participation and cooperation from LUAD patients. This work was supported in part by National Natural Science Foundation of China (82273372, 82203773, 82303450), and the Natural Science Foundation of Jiangsu Province (BK20231233, BK20220250), and the “Qinglan Project” of Jiangsu Province universities, and the Talent Project of Kangda College of Nanjing Medical University (KD2024JXJH001), and Suzhou Key Laboratory for Molecular Cancer Genetics (SZS201209), and Collaborative Innovation Center of Molecular Medicine between Soochow University and Donghai County People's Hospital (H230470), and A Project Funded by the Priority Academic Program Development of Jiangsu Higher Education Institutions (PAPD).

## AUTHOR CONTRIBUTIONS

SW, EJ, and H-TZ contributed to study concept and design. SW, XT, RS, XX, DC, and ZW performed all the experiments. HS, CW, XG, and DH provided technical support. SW, EJ, and H-TZ analyzed the data, wrote the manuscript, and contributed to the interpretation of data and critical revision of the manuscript. SW, XT, and H-TZ provided the funding and supervised the study.

## COMPETING INTERESTS

The authors declare no competing interests.

## ETHICS

Human LUAD tissues were obtained after informed consent was available from all patients. The study protocol was carried out in accordance with the ethical principles outlined in the Declaration of Helsinki and has been approved by the Ethics Committee of Soochow University.

## ADDITIONAL INFORMATION

**Supplementary information** The online version contains supplementary material available at <https://doi.org/10.1038/s41388-026-03752-6>.

**Correspondence** and requests for materials should be addressed to Shengjie Wang, Ersuo Jin or Hong-Tao Zhang.

**Reprints and permission information** is available at <http://www.nature.com/reprints>

**Publisher's note** Springer Nature remains neutral with regard to jurisdictional claims in published maps and institutional affiliations.

Springer Nature or its licensor (e.g. a society or other partner) holds exclusive rights to this article under a publishing agreement with the author(s) or other rightsholder(s); author self-archiving of the accepted manuscript version of this article is solely governed by the terms of such publishing agreement and applicable law.